Sea-to-Air Transfer of Dissolved Organic Carbon via Sea Spray Aerosol during Phytoplankton Bloom

Jie Hu[1], Jianlong Li[1], Narcisse Tsona Tchinda[1], Christian George[2,3], Feng Xu[4], Min Hu[4], and Lin Du[1,2,5,*]

[1]Qingdao Key Laboratory for Prevention and Control of Atmospheric Pollution in Coastal Cities, Environment Research Institute, Shandong University, Qingdao 266237, China

[2]School of Environmental Science and Engineering, Shandong University, Qingdao 266237, China

[3]Universite Claude Bernard Lyon 1, CNRS, IRCELYON, UMR 5256, Villeurbanne F-69100, France

[4]State Key Laboratory of Regional Environment and Sustainability, International Joint Research Center for Atmospheric Research (IJRC), College of Environmental Sciences and Engineering, Peking University, Beijing 100871, China

[5]State Key Laboratory of Microbial Technology, Shandong University, Qingdao 266237, China

Corresponding to: Lin Du (lindu@sdu.edu.cn)

Abstract. The formation of sea spray aerosols (SSA) is linked to wave-breaking events at the sea surface and is widely recognized as an important pathway for the transfer of marine substances to the atmosphere. Although climate change and sea eutrophication have led to the expansion and intensification of coastal phytoplankton blooms, systematic studies on the sea-to-air transfer of dissolved organic carbon (DOC) via SSA during phytoplankton blooms are still lacking, which hinders the understanding of SSA's atmospheric chemistry and climate impacts. In this study, we induced a phytoplankton bloom using coastal seawater and employed various characterization tools to investigate the sea-to-air transfer of DOC. During the phytoplankton bloom, the dynamic accumulation of DOC in coastal seawater leads to fluctuations in the number concentration and mean geometric diameter of SSA by approximately 60% and 30%, respectively; in the meantime, the enrichment factors of DOC in sea surface microlayer, supermicron SSA, and submicron SSA can increase up to ~5-fold, 10-fold, and 30-fold, respectively. The sea-to-air transfer of DOC depends on its selective enrichment as well as the fractionation process at the air-water interface. Interestingly, the particulate property of operationally defined DOC still needs to be considered during SSA formation. Additionally, the sea-to-air transfer of DOC is influenced by the synergistic effects of phytoplankton production and heterotrophic microbial processing, rather than being solely dependent on chlorophyll-a concentration. Compared to previous studies, this work focuses on the sea-to-air interface, systematically and comprehensively elucidating the relationships between DOC's transfer mechanisms, biological activity, and SSA formation. This will further improve our understanding of the ocean-atmosphere carbon cycle and provide insights into its impact on global climate change.

Keywords: sea spray aerosol; dissolved organic carbon; sea-to-air transfer; phytoplankton bloom

1 Introduction

As the largest natural reservoir on Earth, oceans serve as a major source of atmospheric aerosols through the release of

sea spray aerosol (SSA) (Veron, 2015; De Leeuw et al., 2011). Wave-mediated bubble bursting can produce film drops from the retracting bubble film and jet drops from the ejected water column, and they are major components of submicron SSA (<1 μm) and supermicron SSA (≥1 μm), respectively (Wang et al., 2017; Lhuissier and Villermaux, 2012; Jiang et al., 2022). This process will release marine substances into the atmosphere. Since SSA can directly or indirectly scatter solar radiation by acting as cloud condensation and ice nuclei, it has considerable potential for net climate cooling and has therefore been prioritized as a key focus of the marine cloud brightening program (Cochran et al., 2017; Ahlm et al., 2017; Diamond et al., 2022; Feingold et al., 2024). However, there are still significant uncertainties associated with the effects of SSA on climate, particularly in terms of aerosol-cloud interactions. Although substantial efforts have been made to investigate the formation, composition, and properties of SSA, the complexity of natural environment poses challenges to the comprehensive understanding of SSA.

Dissolved organic carbon (DOC) is typically defined as organic matter that can pass through filters, with pore sizes from 0.2 to 0.7 μm, while the retained fraction is termed particulate organic carbon (POC). DOC comprises approximately 66.2% of the total organic carbon in the ocean and is the dominant organic carbon reservoir in the Earth system (Brooks and Thornton, 2018). As the main engine of the ocean's geo-biochemical cycles, microorganisms and their food webs are the primary sources of marine DOC (Quinn et al., 2015). In sunlit surface seawater, phytoplankton production and heterotrophic microbial consumption of organic carbon are particularly active, leading to higher DOC concentrations and faster turnover. At the same time, SSA formation primarily occurs at the seawater surface, meaning that the organic fraction in SSA is closely tied to biological activity. Previous studies have shown that DOC is typically encapsulated as an organic shell around the sea-salt core (Hu et al., 2024; Song et al., 2024). which not only affects the physicochemical properties of the particles (viscosity, surface tension, reactivity, etc.) (Bertram et al., 2018; Tumminello et al., 2024) but also has a profound impact on their climatic effects (cloud condensation activity, ice nuclei activity, and optical properties) (Xu et al., 2022; Christiansen et al., 2020; Vaishya et al., 2013). However, there are still many uncertainties associated with the sea-to-air transfer pattern of DOC via SSA. On the one hand, marine DOC, as a complex mixture, is estimated to consist of 10^{12}–10^{15} organic compounds of varying sizes and chemical classes. The large differences in physicochemical properties among these compounds can lead to different transfer patterns. On the other hand, DOC undergoes more active and complex transformation processes in a more productive surface seawater compared to deeper waters, and there is an unclear relationship between DOC composition and biological activity. Globally, the occurrence of phytoplankton blooms in coastal regions is rapidly expanding and intensifying (Dai et al., 2023). Therefore, elucidating the mechanisms that govern the transfer of DOC from the ocean to the atmosphere will enhance our understanding of related atmospheric chemistry and climatic effects.

In comparison to field observations, laboratory studies offer controlled environments that facilitate the investigation of sea-to-air transfer mechanism of DOC, minimizing the influence of meteorological factors, seawater properties, and external particulate inputs. Previous laboratory simulation studies typically employed simplified modeling systems that focused on a

single organic molecule or class of compounds, overlooking the complexity of DOC and the relationship between DOC composition and biological activity (Schill et al., 2018; Hasenecz et al., 2019; Hartery et al., 2022). Although a few mesocosm experiments have investigated the effects of phytoplankton activity on the physicochemical properties of SSA (Santander et al., 2023; Jayarathne et al., 2022; Wang et al., 2015), the systematical exploration of the sea-to-air transfer pattern of DOC remains insufficient. In this study, we conducted experiments with induced phytoplankton blooms in coastal seawater and used a waterfall type method to simulate the formation of SSA. This study explored the implications of sea-to-air transfer of DOC during phytoplankton blooms. Firstly, the macroscopic effects of phytoplankton blooms on SSA formation and DOC enrichment were examined. Secondly, we employed high-resolution mass spectrometry to analyze the molecular profiles of DOC at different stages of sea-to-air transfer. Finally, by focusing on the most significant contributors, such as proteins, saccharides, and humic substances, the patterns of DOC sea-to-air transfer during phytoplankton blooms were investigated through a micro-to-macro approach.

2 Experimental sections

2.1 Phytoplankton Bloom

Seawater was collected on May 31, 2024, at Shazikou Pier (120°33’28” E, 36°6’37” N) Qingdao, China, and immediately transported to the laboratory. Satellite-derived chlorophyll-a (Chl-a) concentrations indicate that no previous phytoplankton blooms had occurred at the sampling sites (Fig. S1). Details are presented in the Supplement. Seawater was filtered through a 1-mm mesh sieve and transferred into 30 transparent polycarbonate containers, each with a capacity of 28 liters. Guillard’s F/4 medium was added to each container, and these containers were placed outdoors on a flat to promote phytoplankton blooms under natural sunlight (Fig. S2). The phytoplankton bloom experiment began on June 1st, 2024, and lasted for 18 days. To minimize the interference from external environmental factors, these containers remained sealed most of the time. They were shaken at least three times daily, with the caps being briefly opened during each operation to allow ventilation. It is acknowledged that phytoplankton blooms under laboratory conditions may differ from those in natural environments (Jayarathne et al., 2016). During this period, 10 simulation experiments on nascent SSA were conducted. The average diurnal fluctuation in local outdoor air temperature is 3.59 ℃ (temperature average: 21.19 ± 2.60 ℃). Seawater temperature fluctuations in the containers primarily depend on air heat conduction and direct solar heating. However, given seawater’s high specific heat capacity, its diurnal variation is likely smaller than that of air temperature, with an average comparable to air temperature. This value is slightly higher than the 1.04 ℃ diurnal variation (temperature average: 18.72°C ± 1.02 ℃) recorded for coastal seawater in Qingdao during the same period (Cao et al., 2024). Although this temperature discrepancy could influence the development of phytoplankton blooms, it is unlikely to significantly affect the conclusions.

2.2 Generation and Collection of Nascent SSA

In each experiment, three containers of seawater (84 liters) were filtered by 50 μm mesh screen to remove large particles and phytoplankton aggregates and were introduced in our home-made SSA simulation tank (length × width × height = 0.6 × 0.5 × 0.6 m^3). The SSA simulation tank has a design similar to that of the Marine Aerosol Reference Tank, which produces nascent SSA through the plunging waterfall (Stokes et al., 2013). More parameter comparisons are provided in Table S1. Although the intermittent plunging waterfall mode was shown to better reproduce SSA generation, we used a continuous plunging waterfall in order to improve the sampling efficiency of SSA. These two types of plunging waterfalls differ mainly in the behavior of surface bubbles as they rupture and dissipate: in intermittent waterfalls, surface bubbles breaks and dissipates during operational gaps, whereas in continuous waterfalls, surface bubbles gradually dissipates as it moves away from the impact point (Collins et al., 2014). All SSA generation experiments, which typically started around 9:00 AM and lasted for 8 to 9 hours, were conducted at indoor air temperatures (22–25 ℃) that approximate outdoor air temperatures. It is estimated that during this period, the total damage rate to phytoplankton cells in seawater caused by centrifugal pump operation can be significantly lower than 10%. More details on SSA generation and cell damage assessment are provided in the Supplement. Nascent SSA was transported with purified air (Zero Air Supply, Model 111, Thermo Scientific), and the airflow was dried to a relative humidity below 30% (Monotube Dryer, MD700-12F-3, Perma Pure, USA) before collection and measurement. At this relative humidity, nascent SSA can become completely dry. Single particles of SSA were collected by a single particle sampler (DKL-2, Genstar electronic technology Co., Ltd., China) and then analyzed by transmission electron microscopy (TEM, FEI Tecnai G2 F20, Thermo Fisher Scientific, USA). Using a low-pressure cascade impactor (DLPI+, Dekati Ltd., Finland), nascent SSA particles were collected with 14 different particle size classifications (Table S2) and distributed into submicron SSA (0.016-0.94 μm) and supermicron SSA (1.62-10 μm) samples. More information on the schematic diagram of the nascent SSA experiments and the connection between the tank and different samplers is provided in Fig. S3. Since the current study focuses on the sea-to-air transfer of DOC, all SSA samples were extracted with ultrapure water (>18.2 MΩ·cm, 25 ℃, Millipore) and the extractions were filtered with 0.45 μm filters. Further collection details are provided in the Supplement. Blanks were prepared by unexposed quartz fiber filters with the same treatment as for SSA samples.

Prior to the waterfall operation, seawater and sea surface microlayer (SML) samples were collected in SSA simulation tank while maintaining a uniformly mixed and calm state. Seawater was collected at a depth of 10 cm in each container and immediately filtered at low pressure (≤0.2 MPa, avoiding the Chl-a loss) through a GF/F filter (47 mm, Whatman, UK). Both filters and filtered seawater were stored at -20 ℃ in a dark environment. SML was collected in the SSA simulation tank using the glass plate method (Hu et al., 2024). SML samples were filtered through a 0.45 μm filter and then stored in a dark environment at -20 °C. Ultrapure water was treated in the same way as procedural blanks for seawater and SML samples.

2.3 Characterization and Chemical Analysis

2.3.1 SSA Particle Size Distribution

Particle size distributions of dried SSA were measured by a scanning mobility particle sizer (SMPS, GRIMM, Germany) and aerodynamic particle sizer (APS 3321, TSI, USA). SMPS was operated at a sampling flow rate of 0.3 L min^{-1} and a scan rate of 5 min, providing the particle size distribution with electrical mobility diameter (d_{em}) between 0.02 and 1 μm. Aerodynamic particle sizer (APS) detected SSA particles with aerodynamic diameters (d_a) ranging from 0.5 to 10 μm at a scanning rate of 1 min, then paused for 4 min before starting the next scan. Throughout the nascent SSA experiment, both SMPS and APS could provide approximately 90 to 100 results of particle size distribution. The first 4 to 6 results from the initial phase of the experiment were excluded because the SSA number concentration in the headspace of the tank had not yet reached a steady state. The average values were calculated from the remaining results to assess the size distribution characteristics of SSA in the entire experiment. Due to differences in measurement principles, d_{em} measured by SMPS and d_a measured by APS need be converted to the particle's geometric physical diameter (d_p) before they can be merged. Assuming spherical SSA particles, the specific conversion formula is as follows (Eq. (1)) (Harb and Foroutan, 2022; Stokes et al., 2016):

$$d_p = d_{em} = \frac{d_a}{\sqrt{\frac{\rho_{eff}}{\rho_0}}} \quad (1)$$

where ρ_0 is unit density (1.0 g cm^{-3}), and ρ_{eff} is the effective density of the particles (2.0 g cm^{-3}). Since the SSA number concentrations from SMPS and APS are relatively close, we have chosen to merge them around 1 μm.

2.3.2 Chl-a, POC, DOC, Sodium Ion and Surface Tension of Seawater

Quantitative measurements of POC and Chl-a concentrations in seawater were carried out using the GF/F filters described in Section 2.2. Specifically, the concentration of POC in seawater was determined using an elemental analyzer (Elementar, UNICUBE), which measured the POC content in a 1 cm diameter circular area on the GF/F filter. Chl-a in the remaining filters was extracted with 90% (v/v) acetone for 24 h at 4 °C in the dark. Fluorescence values were measured using a Turner Designs 10AU Field Fluorometer (USA), calibrated with chlorophyll standards (Sigma-Aldrich Co.) (Zhong and Ran, 2024; Rocchi et al., 2024), and the values were thereafter converted to Chl-a concentrations in the corresponding volume of seawater. The concentration of DOC was measured by high temperature catalytic oxidation using a total organic carbon (TOC) analyzer (TOC-5000, Metash, China). Measurements were repeated at least 3 times with a relative standard deviation of less than 3%. Sodium ions (Na^+) concentrations were measured using an ion chromatograph (Dionex ICS-600, Thermo Fisher Scientific, USA). The seawater and SML samples were diluted 5,000-fold, while the submicron and supermicron SSA extracts were diluted 5-fold, ensuring that their Na^+ concentrations fall within the 0.1 to 10 μg mL^{-1} range of a seven-point calibration curve for quantification. Repeated measurements confirmed that the relative standard deviation of the Na^+ peak area remained within 6.2%. The surface tension of filtered seawater and SML samples was measured by the platinum plate method using a surface

tension meter (Powereach, JB99B, China). Each measurement was repeated three times, and the average value was taken.

Previous studies have shown that the concentration of Na^+ is typically constant during the sea-to-air transfer. Therefore, the enrichment factor (EF) relative to the concentration of Na^+ can quantify the degree of organic matter enrichment in this transfer (Quinn et al., 2014; Quinn et al., 2015; Jayarathne et al., 2016). It is defined as the concentration ratio of the target substance (X) to that of Na^+ in SSA particles or SML relative to the ratio in seawater (Eq. (2)). Using the uncertainty transfer formula to propagate the uncertainties from multiple measurements results into the calculation of the enrichment factor.

$$EF=\frac{(X)_{SSA\ or\ SML}/(Na^+)_{SSA\ or\ SML}}{(X)_{SW}/(Na^+)_{SW}} \quad (2)$$

2.3.3 Measurements of DOC's Fluorescence

The excitation-emission matrix (EEM) of DOC was obtained using a fluorescence and absorbance spectrometer (Duetta™, Horiba Scientific, Japan). The excitation wavelength of EEM was in the range of 250-620 nm, the emission wavelength was in the range of 250-700 nm, the scanning intervals were set to 5 nm and 2 nm, respectively, and the slit width was fixed at 5 nm. The EEM results for all samples were normalized to Raman units (R. U.) by the Raman peak of water (Ex=350 nm) after subtracting the background signal obtained from Milli-Q water (Chen et al., 2023). EEM data analysis using parallel factor analysis (PARAFAC) with non-negativity constraints were performed with the DOMFlour toolbox by MATLAB R2020a (Stedmon and Bro, 2008). It is important to consider the matrix effects resulting from differences in pH and salinity between seawater samples (seawater and sea surface microlayer) and SSA samples (submicron and supermicron SSA extracts), as well as potential deviations from the variability assumptions of the PARAFAC model due to variations in DOC concentrations across the samples. Therefore, we followed the method outlined by Murphy et al. to normalize each sample's EEMs based on their total signal intensity ((Murphy et al., 2013). After validating the PARAFAC model through split-half verification and random initialization analysis, the normalization was cancelled by multiplying the fractions by each sample's total signal intensity.

2.3.4 Measurements of Saccharides

Saccharides with molecular weight lower than 1 kDa are typically monomers or oligomers consisting of less than five monomers. Due to the high biological turnover, their concentrations represent only 1-2% of DOC in seawater (Kaiser and Benner, 2009), and they are almost undetectable in SSA (Jayarathne et al., 2016). Thus, we focused on saccharides with molecular weight higher than 1 kDa, as these are key components of transparent exopolymer particles, and they constitute most of algae-derived high-molecular-weight (>1 kDa) DOC. Except for the samples collected on Days 1, 9, and 18, samples of submicron SSA, supermicron SSA, SML, and seawater collected on other days were subjected to dialysis for desalting, followed by acid hydrolysis, nitrogen blowing, and re-solubilization (Engel and Händel, 2011). Saccharides were hydrolyzed to monosaccharides, followed by detection using high-performance anion exchange-chromatography with pulsed amperometric detection (HPAEC-PAD, ICS 6000, Dionex), coupled with a Dionex CarboPac PA20 column (2×250 mm) and

a Dionex CarboPac PA20 guard column (2×50 mm). NaOH and sodium acetate (NaAc) were used as mobile phases at a flow rate of 0.250 mL min^{-1}. The detailed gradient elution procedure is shown in Table S3. Identification of the saccharides was based on the retention times of 16 standards (glucose, fructose, xylose, galactose, mannose, trehalose, fucose, rhamnose, arabinose, xylitol, arabinitol, mannitol, galactosamine, glucosamine, galacturonic acid and glucuronic acid). The quantification was performed using seven-point standardized calibration curves with concentrations ranging from 10 nM to 10 μM. According to a previous assessment, the desalting dialysis step retains over 90% of high-molecular-weight DOC (Engel and Händel, 2011); after acidification and hydrolysis, the average recovery rate for most saccharides ranges from 81% to 107%.

2.3.5 Characterization of DOC using Ultra-High Resolution Mass Spectrometry

Based on Chl-a concentration during the phytoplankton bloom, samples of submicron SSA, supermicron SSA, SML, and seawater collected on Day 1, Day 9 (peak of Chl-a), and Day 18 were pretreated for desalting and concentrating using a PPL solid-phase extraction column (100 mg/3 mL, Agilent Technologies). After that, these extractions were then separated for organic compounds using gradient elution on an ultra-high-performance liquid chromatography (UHPLC) system (UltiMate 3000, Thermo Scientific), which was coupled to an LTQ-Orbitrap Velos Pro ETD (Thermo Scientific) operating in ESI- mode to obtain m/z signals from 150 to 1000. Water with 0.1% (v/v) formic acid (eluent A) and acetonitrile (eluent B) was applied for the SSA, SML, and seawater extractions, with a flow rate of 0.3 mL min^{-1}. Gradient elution was performed as follows: eluent B, initially set to 5% for 4 min, increased to 100% in 36 min, was held for 3 min, decreased to 5% in 0.5 min and was held for 12.5 min to recondition the column (Wan et al., 2022). Blank samples were processed using the same procedure. The m/z signals from the corresponding blank samples were subtracted from the aerosol and seawater samples using Xcalibur 4.2.1 software, and the remaining m/z signals were assigned molecular formulas by MFAssignR (R version 4.3.2)(Schum et al., 2020; Radoman et al., 2022). Further details on sample pretreatment, instrumental conditions, and assignment principles are given in the Supplement.

3 Results and discussion

3.1 Variations of Chl-a and DOC during the Phytoplankton Bloom

As an indicator for phytoplankton growth, the time series of Chl-a concentration revealed that a phytoplankton bloom occurred during the experiment (Fig. 1a). The processes of phytoplankton blooms may differ among various outdoor containers, which could limit the consistency of Chl-a concentrations in each container. However, as this study primarily uses seawater in the SSA simulation tank as the liquid medium during nascent SSA experiments, future discussions on Chl-a concentrations (or concentrations of other substances) will focus exclusively on seawater within the SSA simulation tank. The Chl-a concentration increased from 0.48 μg L^{-1} to 36.02 μg L^{-1} on Day 9, and then decreased to a minimum of 6.53 μg L^{-1}. However, the DOC concentration in seawater did not follow the same trend as that of Chl-a, decreasing from 674.9 ± 64.6 μM to 307.39 ± 66.58

μM on Day 5, before increasing again (Fig. 1b). (Biermann et al., 2014)found that the decline in DOC concentration during the early stages of phytoplankton blooms typically ceases after the depletion of inorganic nitrogen and phosphorus in seawater ((Biermann et al., 2014). It has also been reported that the addition of inorganic nutrient not only promotes the heterotrophic consumption of DOC by phytoplankton blooms (Thornton, 2014), but also enhances bacterial production and respiration rates, thereby increasing their ability to utilize DOC(Carlson et al., 2004; Jiao et al., 2010; Cai and Jiao, 2008).

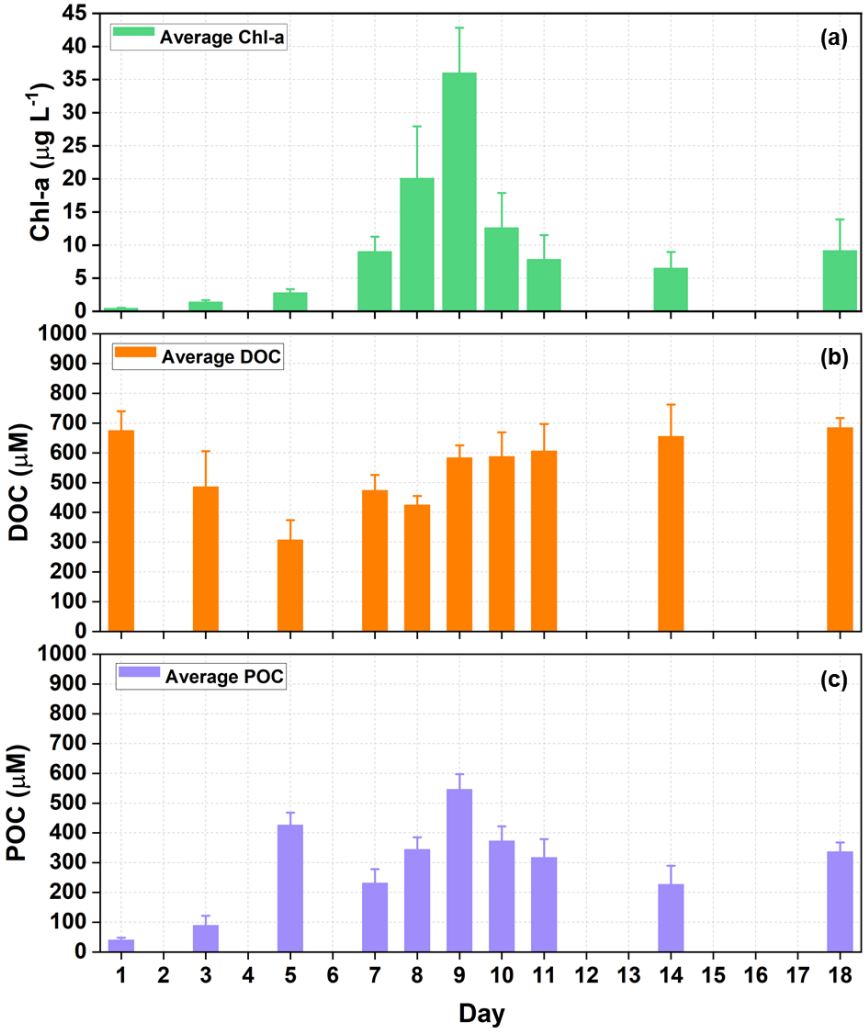

Figure 1. Time series of physicochemical properties of seawater during the phytoplankton bloom. (a) chlorophyll-a (Chl-a), (b) dissolved organic carbon (DOC), and (c) particulate organic carbon (POC) concentrations in seawater. Mean and standard deviations are for three containers of seawater in each experiment.

3.2 Effects of DOC Variations on SSA Formation

3.2.1 Particle Size Distribution of SSA

The distributions of SSA particle size during the phytoplankton bloom are shown in Fig. 2a-b. Prior to Day 10, the production of submicron SSA first decreased, and then increased, while supermicron SSA exhibited an opposite trend. The trend of SSA number concentration closely followed that of submicron SSA, as submicron SSA mainly contributes to the number concentration (Quinn et al., 2015). During the phytoplankton bloom, the geometric mean diameter of SSA increased

from 103.8 ± 5.0 nm on Day 1 to 136.3 ± 5.4 nm on Day 10, before gradually decreasing to 115.0 ± 6.9 nm (Fig. 2c).

The dynamic accumulation of DOC during phytoplankton blooms will have a significant impact on bubble bursting and SSA formation by modifying seawater properties. As an important surface property, surface tension has been proven to be an influential parameter in controlling bubble bursting and SSA formation (Tammaro et al., 2021; Sellegri et al., 2006). The presence of organic matter reduces the surface tension by increasing the average molecular area and weakening hydrogen bonding between water molecules at the air-water interface (Xu et al., 2023). Theoretically, the surface tension of seawater is closely related to the composition and physicochemical properties of the SML. Therefore, the surface tension was measured for the SML samples, with bulk seawater samples taken as controls (secondary formation of the SML within the samples was not considered). In our study, the surface tension of SML exhibited a significant correlation with the number concentration (r = -0.881, $p < 0.01$) and the geometric mean diameter ($r = 0.929$, $p < 0.01$) of SSA. As shown in Fig. 2d, the surface tension of SML sample at the start of the experiment was measured at 65.84 ± 0.36 mN m^{-1}, which exceeded our expectations. Using both primary and secondary mass spectrometry, we detected diethyl phthalate in the SML on Day 1 (Fig. S4). As common plasticizer, it is often found in coastal seawater and accumulates in SML due to its low solubility and hydrophobic nature (Lu et al., 2023), significantly reduce surface tension even at low concentrations (Fig. S5). However, no diethyl phthalate was detected in bulk seawater sample on Day 1, which suggests that they likely do not influence phytoplankton blooms in bulk seawater. Detailed mass spectrometry and source analysis can be found in the Supplement. Surface tension of the SML increased rapidly during the initial phase, being potentially associated with declining concentrations of diethyl phthalate. This compound was undetectable in the SML sample on Day 9, which could result from the biosorption or transformation by marine microorganisms (Liang et al., 2024; Gao and Chi, 2015). Previous studies have explored the relationship between surface tension and the formation of SSA by adding surfactants at varying concentrations (Sellegri et al., 2006; Tyree et al., 2007; Song et al., 2024). Our findings also indicate that changes in surface tension during phytoplankton blooms play a key role in influencing the formation of SSA. It was reported that increased surface tension tends to inhibit the instability of bubble film edge and the development capillary waves during bubble bursting, thereby reducing the number of film drops and increasing the droplet size (Wang and Liu, 2025; Lhuissier and Villermaux, 2012). In coastal waters where surfactants are abundant, surface tension changes are similar to those observed in SML during phytoplankton blooms may be widespread. Biologically induced DOC fluctuations will directly affect the particle size distribution of SSA, ultimately affecting SSA behavior such as atmospheric residence time and wet/dry deposition (Veron, 2015).

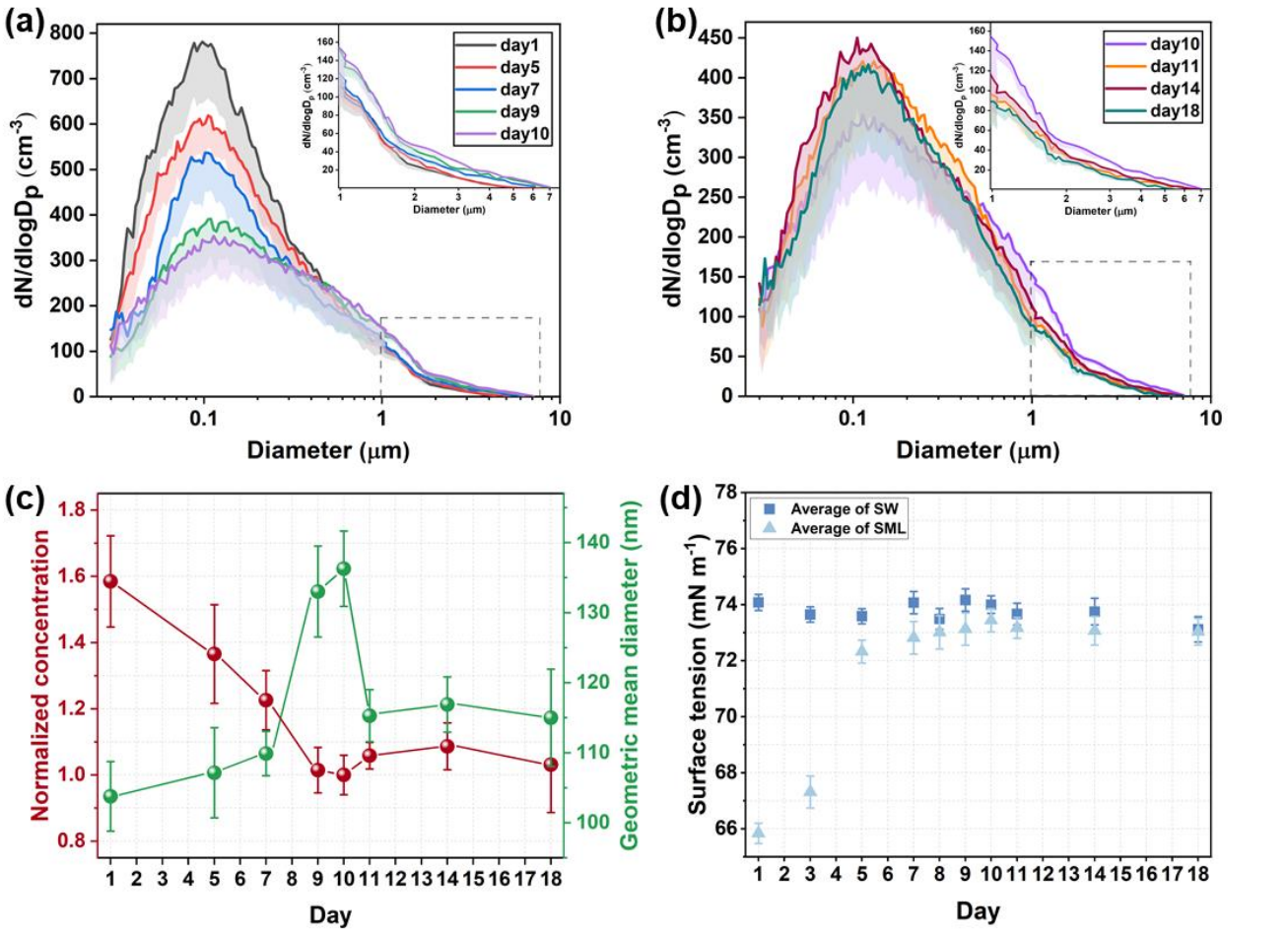

Figure 2. Time series of SSA formation during the phytoplankton bloom. (a) Particle size distributions of SSA from Day 1 to 10; (b) Particle size distributions of SSA from Day 10 to Day 18. For clarity, the gray dashed box area is the result of the aerodynamic particle sizer and is enlarged to the upper right corner. Shading is the standard deviation in the negative direction. (c) Number concentrations and geometric mean diameters of SSA. Error bars are standard deviations for SSA size distribution results measured by SMPS and APS at 5-minute intervals during the nascent SSA sampling period. (d) Surface tension of SML and bulk seawater. Error bars are the standard deviation of three repeated measurements.

3.2.2 Enrichment Factor of DOC in SSA

During the phytoplankton bloom, DOC's variations not only directly influence SSA particle size distribution, but also significantly affect the enrichment of organic matter within SSA. Due to the limited SSA collection, samples on Day 1, Day 9, and Day 18 were not analyzed for the EF of DOC and were only used for subsequent mass spectrometry analysis. In our phytoplankton bloom experiments, the EFs of DOC in SML, supermicron SSA, and submicron SSA increased by up to ~5-fold, 10-fold, and 30-fold, respectively. The highest EF in the SML was observed on Day 5, during which the increase in the EF of DOC was not contradictory to the increase in surface tension of the SML samples. The rise in surface tension of the SML samples could be attributed to a reduction in a highly surface-active organic pollutant. However, because its concentration is extremely low (below 2 μM, seeing Fig. S5), it does not significantly impact the EF of the DOC (ranging from 700 to 2200

μM C) in the SML samples. Carbon isotope studies indicate that the SML functions as a "pre-enrichment" zone for DOC enriching into SSA, especially for submicron SSA (Crocker et al., 2022). However, the highest EFs in submicron and supermicron SSA were on Day 7 (given the low EF of DOC in the SML on Day 9, it is unlikely that DOC's EF in SSA at this time would reach its highest value), and the morphological structural images of SSA also illustrate a significant enhancement in DOC enrichment (Fig. S6). The time series of DOC's EF in the SML and SSA do not align, indicating that the sea-to-air transfer of DOC is likely to be complex. Temporal fluctuations in DOC compositions and concentrations triggered by biological cycles during phytoplankton blooms may play an important role in influencing DOC's sea-to-air transfer. Compared to supermicron SSA, the EF of DOC in submicron SSA consistently exhibited higher values and faster increases, which may be attributed to differences in SSA formation mechanisms. Before the bubble film ruptures at the water surface, gravity continuously expels the liquid within it, while surface-active substances, being lighter, are pushed upward, forming a vanishingly thin film (Lhuissier and Villermaux, 2012). The resulting film drops are thus enriched with a higher concentration of organic matter. In contrast, jet drops primarily originate from the liquid at the air-water interface inside the bubble and are typically less enriched in organic matter than film drops (Crocker et al., 2022).

Compared to particle size distribution, the significant variation in DOC's EF in SSA may have more profound implications for SSA's climate effects. The widely reported phenomenon of organic matter enveloping inorganic salt cores (as illustrated in Fig. S6) significantly influences the cloud condensation nucleation activity (Bates et al., 2020; Lee et al., 2020; Cravigan et al., 2020) and ice nucleation activity of SSA (Pandey et al.; Hartmann et al., 2025), with specific effects depending on the type of organic matter. Although the EF of DOC in SSA reflects the overall characteristics of sea-to-air transfer pattern, more detailed studies are still needed to elucidate the specific pattern of different organic species.

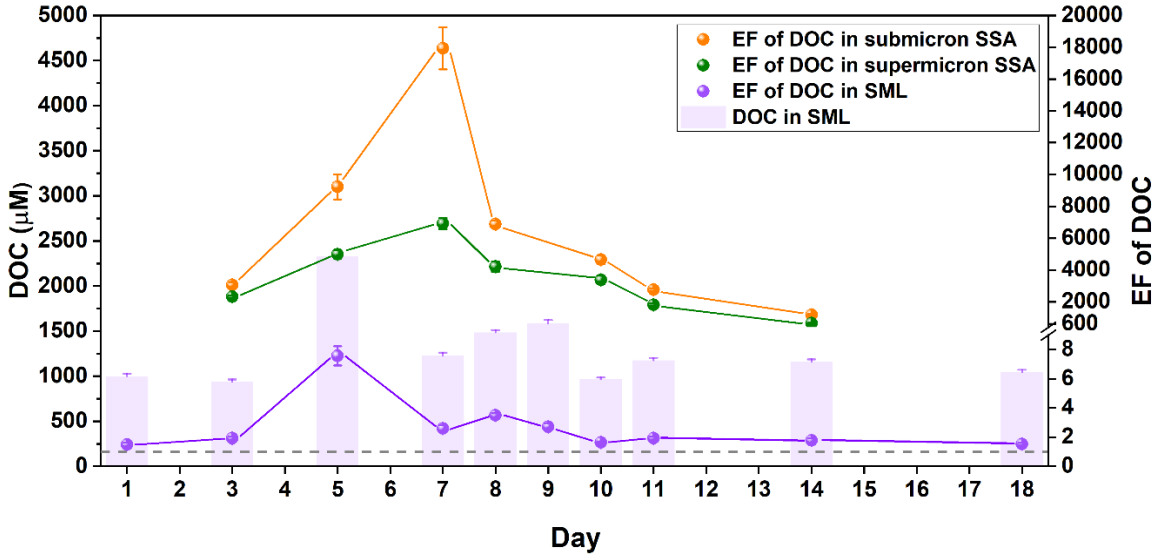

Figure 3. Time series of DOC enrichment during the phytoplankton bloom. Enrichment factors of DOC relative to Na^+ in the SML (purple), submicron SSA (orange) and supermicron SSA (green). Error bars represent the deviation of the EF, derived from the standard deviation of Na^+ concentration and DOC concentration obtained through two repeat measurements. The

purple column is the concentration of DOC in the SML, and the error bars are derived from at least three repeated measurements.

3.3 Exploring the Sea-to-Air Transfer of DOC

3.3.1 Overview of Organic Molecules during the Sea-to-air Transfer

To investigate the link between the sea-to-air transfer of DOC and biological activity, samples of submicron SSA, supermicron SSA, SML, and seawater were collected on Day 1, Day 9 (peak of Chl-a) and Day 18 for mass spectrometry analysis. Molecular formula assignments of m/z lists from different samples were carried out using MFAssignR. The molecules were categorized into CHO, CHNO, CHOS, and CHNOS groups and plotted in van Krevelen diagrams (Fig. S7). Among the different samples, the most prevalent molecular formulas were from the CHO and CHNO groups, which accounted for (23.19 ± 3.34) % and (63.49 ± 4.52) % of the total number of assigned molecular formulas, and (27.94 ± 7.53) % and (65.17 ± 8.18) % of the total intensity of assigned molecular formulas, respectively (Fig. 4a). Compared to Day 1 and Day 18, the differences in the number and intensity of assigned molecular formulas between submicron and supermicron SSA are greater on Day 9, primarily due to CHNO-type molecular formulas. The same conclusion can also be found in SML and seawater. DOC molecules exhibited a higher intensity-weighted average value of H/C and a lower value for O/C on Day 9 (Table S4), which indicates that more low-oxidized and hydrophobic organic matter enriched in the SML.

Fig. 4b presents Venn diagrams that illustrate the number of assigned molecular formulas in the four sample types, with the intersections indicating shared molecular formulas. Submicron SSA and the SML showed greater molecular similarity (33.2 ± 7.8) %, and the highest percentage of identical molecular formulas was observed at 41.7% on Day 9. These reflect that the SML, as a crucial region for air-water interface fractionation of DOC, serves as an important source of DOC in submicron SSA. As shown in Fig. 4a, the total intensity of molecular formulas assigned to seawater remained relatively stable across the three stages of the phytoplankton bloom, while the total number exhibited a stepwise decline. This suggests that the composition of DOC in seawater is influenced by biological activity during phytoplankton blooms (Meon and Kirchman, 2001), which in turn affects the sea-to-air transfer of DOC via SSA (Schmitt-Kopplin et al., 2012). For instance, our results show that the proportion of shared organic molecular formulas in SW, SML, submicron SSA, and supermicron SSA was 12.4% on Day 1, 16.2% on Day 9, and significantly increased to 26.3% on Day 18.

Based on the van Krevelen diagrams (Fig. S8) and a more detailed division rule (Fig. S6), the assigned molecular formulas in the different samples and their groups (CHO, CHNO, CHOS, and CHNOS) can be further allocated into seven biochemical categories (Suo et al., 2024; He et al., 2023). As illustrated in Fig. 4c, lipid-like, protein-like, carbohydrate-like and lignin-like molecules accounted for the majority of organic molecules transferred from sea to air. A previous study has suggested that the DOC produced by algae consists of two major aliphatic groups: proteins and saccharides (Suo et al., 2024). Lignin-like molecules are widely considered to predominantly contribute to humic substances (Kim et al., 2003; Labeeuw et al., 2015). However, considering the effects of ionization mode and ionization efficiency, mass spectrometry results cannot directly reflect

the relative abundance or concentration changes of specific DOC species. Therefore, additional methods were used to quantify the concentration fluctuations of protein, saccharides and humic substances in DOC to better understand the link between DOC's sea-to-air transfer and biological activity.

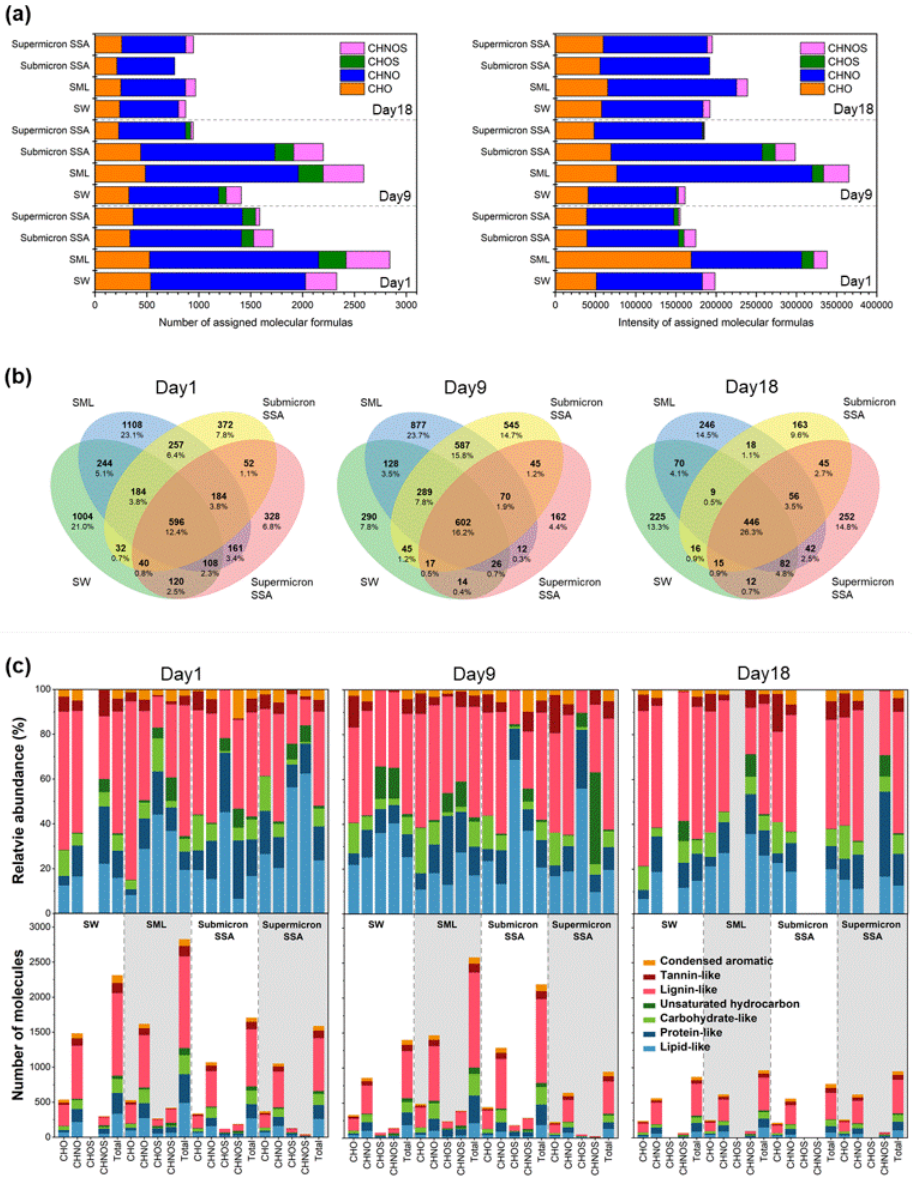

Figure 4. Sea-to-air transfer of organic molecules. (a) The number and intensity of molecular formulas assigned in different samples. (b) Venn diagram illustrating the number of assigned molecular formulas. Percentages represent the proportion of molecules in each region relative to the union set. (c) Relative abundance and molecular number contributions of the seven molecular types derived from the Van Krevelen diagrams. The gray background is for visual differentiation purposes only.

3.3.2 Selective Enrichment and Interfacial Fractionation: A Perspective of Proteins and Humic Substances

By EEM-PARAFAC method (Fig. 5a), three fluorescence compounds co-exiting in seawater, SML, submicron SSA, and supermicron SSA were identified. The peaks of protein-like substances (PRLIS) are mainly at (280 nm)/ (330 nm), and most of them were due to tryptophan-like substances (Santander et al., 2022). The humic-like substances (HULIS) peaks mainly

appear at the excitation/emission wavelengths of (<245 nm or 320 nm)/ (396 nm) for HULIS 1, and at (260 or 360 nm)/ (450-455 nm) for HULIS 2. The production of HULIS 1 is primarily linked to heterotrophic processes, whereas HULIS 2 is a photooxidation product and, as such, contains a higher oxygen content than HULIS 1 (Santander et al., 2023; Barsotti et al., 2016).

The EEM intensities of PRLIS, HULIS 1, and HULIS 2 in seawater, sea surface microlayer, submicron SSA, and supermicron SSA are shown in Fig. 5b. To exclude the correlation between EEM intensities in SSA samples and the mass of collected SSA, we standardized the EEM intensities using Na^+ concentration. During phytoplankton blooms, HULIS 1 and HULIS 2 gradually accumulated in seawater, while PRLIS initially increased and then decreased. The EEM intensity of PRLIS was significantly stronger than that of HULIS 1 and HULIS 2 in the SML, submicron SSA, and supermicron SSA. PRLIS includes small peptide molecules and soluble amino acids formed from the degradation of cells, cellular debris, or large proteins. Due to their hydrophilic groups (-NH_2 and -COOH) and hydrophobic carbon chains, they have been reported to exhibit strong enrichment potential in the SML and SSA (Triesch et al., 2021a; Triesch et al., 2021b). As shown in Fig. 5b, the EEM intensity of PRLIS in SSA rapidly peaks on Day 7 before declining. This pattern closely aligns with the DOC's enrichment factor trend in SSA presented in Fig. 3, indicating that PRLIS was the primary contributor to the increase of DOC's EF during the phytoplankton bloom. As a less oxidized organic matter, HULIS 1 exhibited a greater enrichment capacity in SSA than HULIS 2. Consequently, HULIS1 have greater abundance in the SML and SSA compared to HULIS2 (Fig. 5c). Compared to supermicron SSA, the EEM intensities of the three organic compounds in submicron SSA is higher. Compared to supermicron SSA, the EEM intensities of the three organic compounds are higher in submicron SSA. Consistent with previous studies, besides the properties of the organic matter itself, the sea-to-air transfer of DOC is also influenced by the different generation mechanism of SSA (Crocker et al., 2022).

The correlations between organic carbon concentration and the three fluorescent compounds during sea-to-air transfer were further explored. We found that the EEM intensities of the three compounds in seawater are positively correlated with the DOC concentration, while in the SML, these compounds are significantly positively correlated with the POC concentration in seawater. This implies that DOC in the SML might mainly originate from POC in seawater. Within the same type of samples (seawater, SML, submicron SSA, or supermicron SSA), PRLIS, HULIS 1, and HULIS 2 often maintained significant positive correlations; however, when sample types differ, significant correlations between them are rarely observed (Fig. 5d). In seawater and SML samples, the non-significant correlation may be due to the fact that these three organic fractions originate from different organic carbon pools in seawater. For submicron and supermicron SSA, the non-significant correlation may result from DOC undergoing different air-water interfacial fractionation processes (Quinn et al., 2015). The concentration variations of DOC resulting from multiple enrichment processes at different air-water interfaces may obscure its consistency with the concentration variations induced by microbial activity in seawater. Typically, DOC in submicron SSA undergoes more pronounced interfacial fractionation than DOC in supermicron SSA (Crocker et al., 2022). Another factor that may reduce the

correlation among the samples is the time lag in the sea-to-air transfer. For instance, PRLIS peaked on Day 5 in the SML, while it peaked on Day 7 in submicron SSA. This lag could be related to bacterial activity or may be limited by the size of the DOC in the SML, which will be better illustrated in the next section on saccharides.

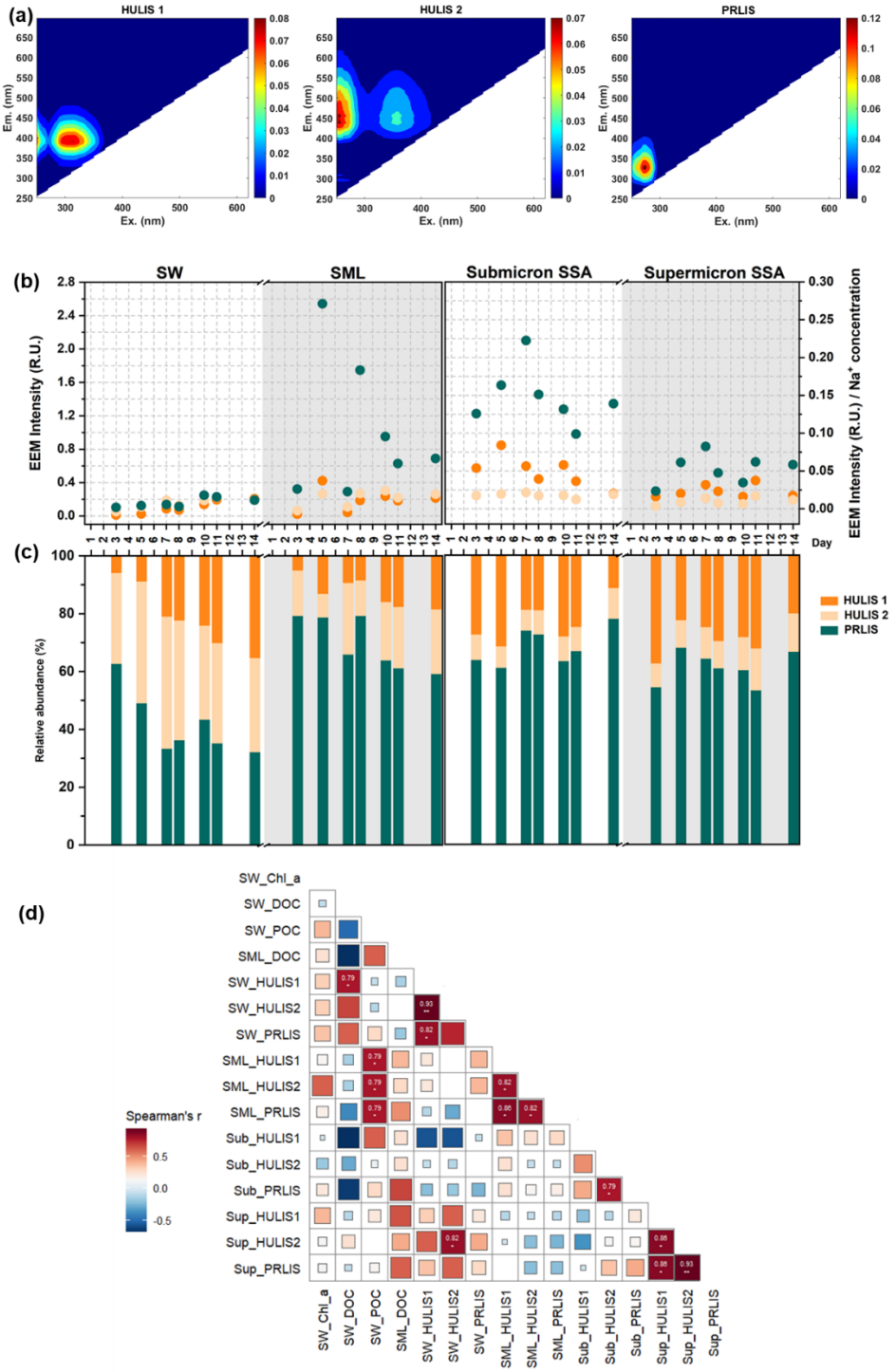

Figure 5. Sea-to-air transfer of HULIS and PRLIS. Three organics identified using the EEM-PARAFAC method: (a) HULIS 1, HULIS 2, and PRLIS. (b) EEM intensities of the three organics in different samples with respect to time. Note that in order to exclude the effect of SSA collection mass on EEM intensity, EEM intensities of SSA samples were normalized with their Na^+ concentrations. (c) Relative abundance of EEM intensities of the three organics in different samples with respect to time. (d) Spearman's correlation between Chl-a, DOC and POC concentrations in seawater, POC concentration in the SML and EEM

intensities of three fluorescent substances.

3.3.3 Bacterial Modification and Size Limitation: A Perspective of Saccharides

Phytoplankton typically sequesters the excess carbon as saccharides in energy storage materials, cell walls, and extracellular polysaccharides, and this process is influenced by phytoplankton growth, heterotrophic bacteria, and environmental conditions (Mühlenbruch et al., 2018). The accumulation of saccharides in seawater and phytoplankton growth processes is interrelated but not fully synchronized. In both seawater and SML, two distinct peaks in total saccharides were observed, occurring before and after the peak of Chl-a concentration (Fig. 6a). It has been reported that under inorganic nutrient-sufficient conditions, the high metabolic activity of phytoplankton during the exponential growth phase leads to the secretion of large amounts of extracellular polysaccharides, which rapidly aggregate into highly viscous, transparent exopolymer particles (TEP), thereby promoting phytoplankton clustering (Passow, 2002; Villacorte et al., 2015). The direct conversion of DOC into TEP by bacteria during the early stage of phytoplankton blooms also represents an important pathway for TEP production (Engel et al., 2004; Passow, 2002). Since added inorganic nutrients were depleted on Day 5, phytoplankton is likely to adjust its metabolism, leading to reduced extracellular polysaccharide secretion, while enhancing bacterial degradation of saccharides (Passow, 2002). A second peak in saccharide concentration occurring on Day 11, is attributed to the collapse of the phytoplankton bloom, which releases intracellular saccharides and causes a temporary rise in its concentration in seawater (Mühlenbruch et al., 2018).

As shown in Fig. 6b, the total saccharide concentration accounted for 32.84 ± 10.02 % of DOC in seawater and 28.23 ± 18.00 % of DOC in the SML. The bacterial activity was indicated by the ratio of the sum of fucose and rhamnose concentrations to the sum of arabinose and xylose concentrations, with ratios below 1 indicating high bacterial concentrations (see the black scattered points in Fig. 6b) (Jayarathne et al., 2022). Seawater and SML exhibit different time series of bacterial activity, suggesting that they may harbor distinct microbial communities (Rahlff et al., 2023; Rahlff et al., 2019; Reinthaler et al., 2008). The rapid increase in the percentage of saccharides in the SML after Day 10 was accompanied by an increase in bacterial activity within the SML. This increase in saccharide percentage can be attributed, on one hand, to the release of saccharides from phytoplankton die-off, and on the other hand, to a decrease in PRLIS concentration in the SML (Fig. 5b), which reduced the competition for saccharides to be enriched at the interface. However, the percentage of saccharides in SSA remained consistently below 10%, with a significant increase only observed on Day 14, corresponding to the peak bacterial activity in the SML. Hasenecz et al. found that addition of heterotrophic bacteria significantly increased the saccharide enrichment in SSA, as the enzymes released by these bacteria further modified the saccharides further (Hasenecz et al., 2020). The time lag in the increase of saccharide percentage from seawater to SSA through SML indicates that bacterial modifications are crucial in the sea-to-air transfer of saccharides.

Saccharides are more abundant in seawater and the SML, with nearly all of the 16 monosaccharides/disaccharides

detectable in the hydrolyzed products of polysaccharides (Fig. 6c). Due to the interconnectivity between seawater and SML, their saccharide compositions show good similarities. However, the varying fractionation behaviors of saccharides during the sea-to-air transfer led to a reduction in their diversity in SSA. Glucose, mannose, and xylose emerged as the most relatively abundant saccharides in SSA, with corresponding EFs being the highest in both submicron and supermicron SSA (Fig. S9). In contrast to some simplified experimental model systems (Xu et al., 2024; Hasenecz et al., 2019). the EFs of saccharides in submicron and supermicron SSA do not show the expected differences in our experiments (Fig. S7). Furthermore, a substantial variability exists in the EFs among different saccharides. We suggest that the size limitations of saccharides should be considered during the sea-to-air transfer via SSA, despite their operational definition as DOC (<0.45 μm).

According to the bubble-mediated mechanism of SSA formation, the size of polysaccharides may play a key role in their enrichment in SSA. Regardless of whether the film drops are generated by Rayleigh-Taylor (Lhuissier and Villermaux, 2012) or Squire instability (Jiang et al., 2022), we believe that the main prerequisite for polysaccharides to enter the film drops is their consistent presence in the bubble film, at least until it ruptures. For bubbles with radius of ~1 mm, the bubble film thickness can reduce to around ~100 nm at rupture (Lhuissier and Villermaux, 2012). However, bubbles with radius smaller than ~1 mm dominate the number concentration (Stokes et al., 2013), and their bubble film will be thinner at rupture. A similar theory applies to the generation of jet drops: the “liquid layer” (the thickness of which is determined by viscous, inertial, and surface tension forces) (Ji et al., 2022) located at the air-water interface inside the bubble needs to hold the polysaccharide until the cavity collapses to form jet drop.

Generally, polysaccharides that can be enriched in film drops are smaller in size compared to those enriched in jet drops, due to the thinner bubble film and smaller film drop. The size of saccharides is partially determined by their functionality. Glucose and fructose are important monosaccharides that constitute cellular energy storage substances (glucan and fructan), and it is reported that the majority of these polysaccharides have sizes smaller than 6 nm in phytoplankton blooms (Hasenecz et al., 2020). Therefore, they exhibit higher EFs in both submicron and supermicron SSA (Fig. S

). For a specific type of polysaccharide, if its size does not meet the conditions for entry into film drops but does for jet drops, it is reasonable to observe its greater EF in jet drops than in film drops. For example, our experimental results showed that fucose was scarcely detected in submicron SSA, but was only enriched in the SML and supermicron SSA. Previous studies indicate that fucose-constituted polysaccharides primarily range from 50 nm (≈100 kDa) to 450 nm, representing a relatively large size (Jayarathne et al., 2022). It was also suggested that these polysaccharides resist bacterial hydrolysis (Murray et al., 2007). This may explain why these polysaccharides did not effectively enter the submicron SSA during our experimental period. Saccharide alcohols, including xylitol, arabinitol, and mannitol, make up less than 5% of the total saccharides. These compounds are effective osmoregulatory substances that help phytoplankton cells adapt to their environment. They may also result from bacterial decomposition of organic matter, typically in the free state or as low molecular weight forms (Jayarathne et al., 2022; Pramanik et al., 2011), and can be enriched in SSA. Glucuronic and galacturonic acids are the main components

of bacterial extracellular polysaccharides but they make up only a small percentage of those of phytoplankton (Zhang et al., 2015; Bhaskar and Bhosle, 2005). Since the polysaccharides produced by these bacteria are much less bioavailable, they are difficult to efficiently degrade by bacterial enzymes into smaller molecular weights (Mühlenbruch et al., 2018), which may inhibit their sea-to-air transfer.

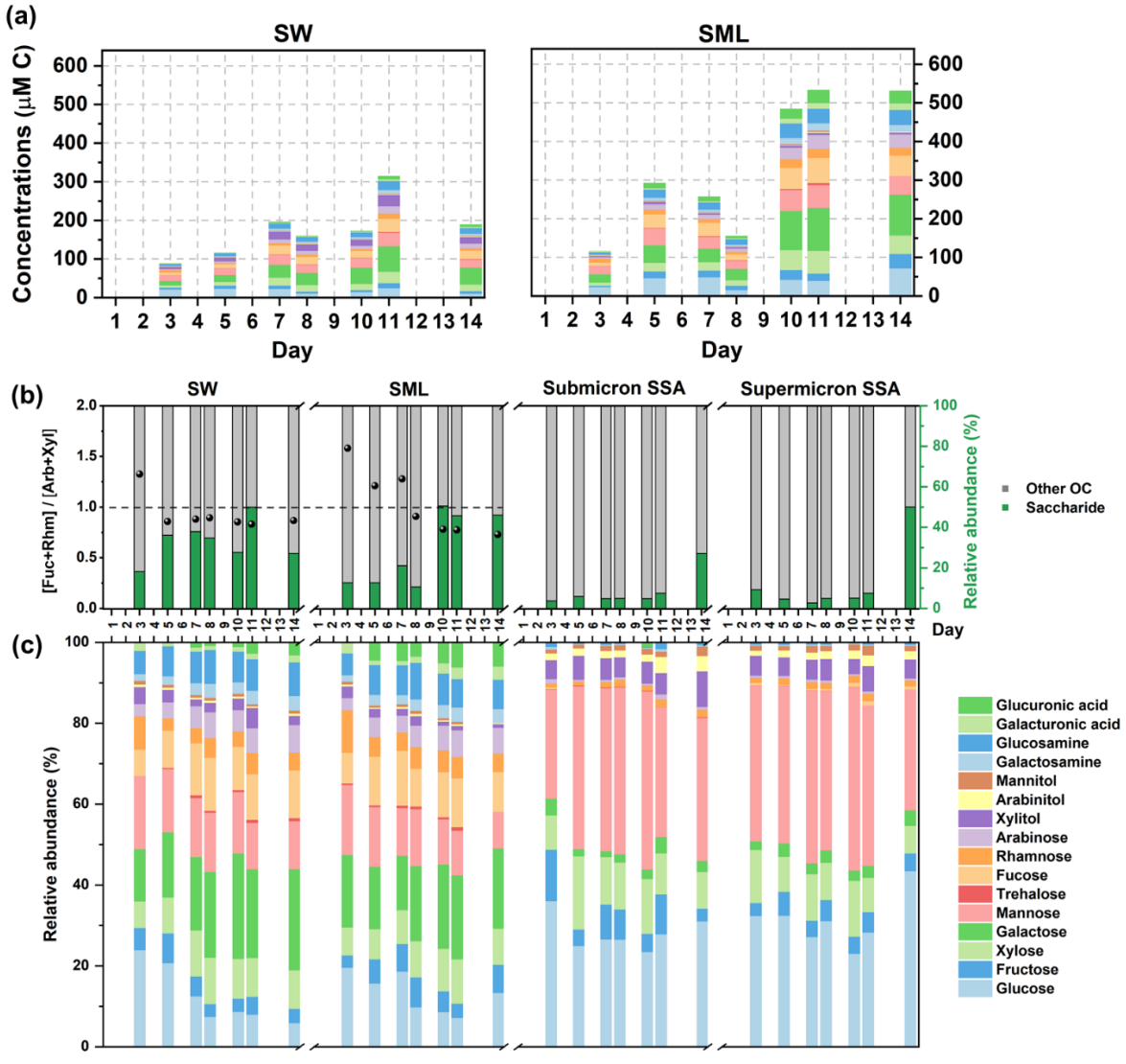

Figure 6. Sea-to-air transfer of saccharides. (a) Relative abundance of total saccharides in DOC. The bacterial activity is expressed as the ratio of the sum of the concentrations of fucose and rhamnose to the sum of the concentrations of arabinose and xylose (the black scatters). The activity is typically considered higher when the ratio is less than 1. (b) Composition and relative abundance of saccharides.

4 Atmospheric implications

Phytoplankton blooms are “pulse events” in ocean-atmosphere organic carbon cycle, transferring functionally specific molecules through SSA to the atmosphere, and potentially influencing cloud condensation nucleation and the atmospheric chemistry of SSA. In this study, we found that DOC enrichment in SSA during phytoplankton blooms can increase by up to

10-30 times, and this promoting effect resulted from the coupling of biological activity and "DOC-Bubble-SSA" interactions (Fig. 7). First, biological activity-driven organic carbon cycling in seawater triggers fluctuations in DOC concentration and composition. The dynamic accumulation of DOC directly influences SSA formation by altering the physical properties of seawater surfaces and indirectly impacts the sea-to-air transfer of DOC via SSA. Secondly, due to the varying enrichment capacities of different organic components in SSA, the changes in DOC composition and concentration in seawater caused by phytoplankton blooms are a key factor in the time-series fluctuations of the DOC enrichment factors. Finally, DOC produced by phytoplankton cannot immediately transfer to SSA and often requires modification by heterotrophic microorganisms before effective transfer. Note that size constraints on operationally defined DOC (<0.45 μm) exist for the enrichment both in film drops and jet drops, with more stringent size constraints for film drops. Overall, proteins appear to be the main contributors to DOC sea-to-air transfer during the phytoplankton bloom, while the contribution of saccharides increased significantly only towards the end of the bloom. Polysaccharides and amino acids produced by phytoplankton have been demonstrated to be key substances for efficient ice nucleation activity and are frequently detected in SSA and low-level clouds (Triesch et al., 2021a; Triesch et al., 2021b; Hartmann et al., 2025). Therefore, given the frequent occurrence of phytoplankton blooms and the enhancing effect of ocean warming, they will ultimately exert a profound influence on climate through the sea spray process.

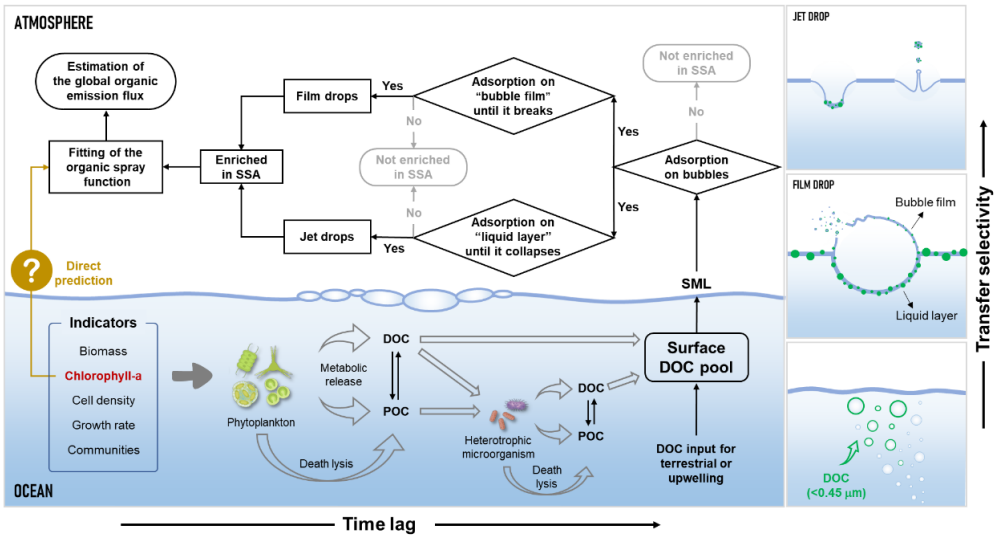

Figure 7. Sea-to-air transfer patterns of DOC via SSA during phytoplankton blooms.

Although there are ongoing debates about the effectiveness of Chl-a concentrations in predicting the organic spray emissions (O'dowd et al., 2008; Bates et al., 2012; Rinaldi et al., 2013; Quinn et al., 2014), it can be asserted that Chl-a, as readily available from global satellite data, remains essential in these predictions, especially when it is constrained with appropriate parameters. The current study indicates that Chl-a is a driven factor to regulating the sea-to-air transfer of DOC. However, the influence of microbial cycling and SSA formation mechanisms complicates this regulatory role, preventing it from manifesting as a straightforward linear relationship. For the future organic spray emission models, it is advisable to incorporate time-series variations in Chl-a concentrations, as they could reflect the progression of phytoplankton blooms. Additionally, careful consideration should be given to dividing different biogeochemical ocean regions, which includes

identifying both Chl-a concentration control regions (O'dowd et al., 2008) and non-control regions (Quinn et al., 2014), to enhance the spatiotemporal resolution.

Data availability

The data in our study are available from the corresponding author on reasonable request.

Supplement

Additional experimental details, materials and methods, including description of experimental apparatus, sample collection and detection, SSA morphology and chemical composition, and calculation methods and results.

Author Contributions

J. H., L. D. and J. L. designed and conceived the research; J. H. and F. X. conducted the experiments; J. H. performed data analysis; J. H. and J. L. wrote the original draft paper; N. T. T., C. G., M. H. and L. D. helped to write, review, and edit the manuscript.

Competing interests.

The contact author has declared that none of the authors has any competing interests.

Acknowledgements

We would like to thank Xiangmei Ren, Shunni Dong from State Key Laboratory of Microbial Technology of Shandong University for help and guidance in HPIC. We would like to thank Xiaoju Li from State Key laboratory of Microbial Technology of Shandong University for help and guidance in TEM.

Disclaimer

Publisher's note: Copernicus Publications remains neutral with regard to jurisdictional claims made in the text, published maps, institutional affiliations, or any other geographical representation in this paper. While Copernicus Publications makes every effort to include appropriate place names, the final responsibility lies with the authors.

Financial support

This work was supported by National Natural Science Foundation of China (22376121, 22361162668 and 42476033), National Key Research and Development Program of China (2023YFC3706203), and Intramural Joint Program Fund of State Key Laboratory of Microbial Technology (SKLMTIJP-2025-02).

References

Ahlm, L., Jones, A., Stjern, C. W., Muri, H., Kravitz, B., and Kristjánsson, J. E.: Marine cloud brightening – as effective without clouds, Atmos. Chem. Phys., 17, 13071-13087, https://doi.org/10.5194/acp-17-13071-2017, 2017.

Barsotti, F., Ghigo, G., and Vione, D.: Computational assessment of the fluorescence emission of phenol oligomers: A possible insight into the fluorescence properties of humic-like substances (HULIS), J. Photoch. Photobio. A, 315, 87-93, https://doi.org/10.1016/j.jphotochem.2015.09.012, 2016.

Bates, T. S., Quinn, P. K., Coffman, D. J., Johnson, J. E., Upchurch, L., Saliba, G., Lewis, S., Graff, J., Russell, L. M., and Behrenfeld, M. J.: Variability in Marine Plankton Ecosystems Are Not Observed in Freshly Emitted Sea Spray Aerosol Over the North Atlantic Ocean, Geophys. Res. Lett., 47, e2019GL085938, https://doi.org/10.1029/2019GL085938, 2020.

Bates, T. S., Quinn, P. K., Frossard, A. A., Russell, L. M., Hakala, J., Petäjä, T., Kulmala, M., Covert, D. S., Cappa, C. D., Li, S. M., Hayden, K. L., Nuaaman, I., McLaren, R., Massoli, P., Canagaratna, M. R., Onasch, T. B., Sueper, D., Worsnop, D. R., and Keene, W. C.: Measurements of ocean derived aerosol off the coast of California, J. Geophys. Res. Atmos., 117, http://doi.org/10.1029/2012JD017588, 2012.

Bertram, T. H., Cochran, R. E., Grassian, V. H., and Stone, E. A.: Sea spray aerosol chemical composition: elemental and molecular mimics for laboratory studies of heterogeneous and multiphase reactions, Chem. Soc. Rev., 47, 2374-2400, https://doi.org/10.1039/C7CS00008A, 2018.

Bhaskar, P. V. and Bhosle, N. B.: Microbial extracellular polymeric substances in marine biogeochemical processes, Curr. Sci., 88, 45-53, https://www.jstor.org/stable/24110092, 2005.

Biermann, A., Engel, A., and Riebesell, U.: Changes in organic matter cycling in a plankton community exposed to warming under different light intensities, J. Plankton Res., 36, 658-671, https://doi.org/10.1093/plankt/fbu005, 2014.

Brooks, S. D. and Thornton, D. C. O.: Marine Aerosols and Clouds, Annu. Rev. Mar. Sci., 10, 289-313, https://doi.org/10.1146/annurev-marine-121916-063148, 2018.

Cai, H. and Jiao, N.: Diversity and Abundance of Nitrate Assimilation Genes in the Northern South China Sea, Microb. Ecol., 56, 751-764, https://doi.org/10.1007/s00248-008-9394-7, 2008.

Cao, L., Qiu, Y., Xue, L., Zhang, Y., Zhang, S., Wu, N., Yuan, D., Li, Q., Zhao, Z., Wang, N., Zhou, Y., Yang, W., Li, C., and Liu, Y.: Sea surface carbon dioxide during early summer at the Tuandao nearshore time series site, Mar. Environ. Res., 201, 106699, https://doi.org/10.1016/j.marenvres.2024.106699, 2024.

Carlson, C. A., Giovannoni, S. J., Hansell, D. A., Goldberg, S. J., Parsons, R., and Vergin, K.: Interactions among dissolved organic carbon, microbial processes, and community structure in the mesopelagic zone of the northwestern Sargasso Sea, Limnol. Oceanogr., 4, 1073, https://doi.org/10.4319/lo.2004.49.4.1073, 2004.

Chen, H., Yan, C., Fu, Q., Wang, X., Tang, J., Jiang, B., Sun, H., Luan, T., Yang, Q., Zhao, Q., Li, J., Zhang, G., Zheng, M., Zhou, X., Chen, B., Du, L., Zhou, R., Zhou, T., and Xue, L.: Optical properties and molecular composition of wintertime atmospheric water-soluble organic carbon in different coastal cities of eastern China, Sci. Total Environ., 892, 164702, https://doi.org/10.1016/j.scitotenv.2023.164702, 2023.

Christiansen, S., Ickes, L., Bulatovic, I., Leck, C., Murray, B. J., Bertram, A. K., Wagner, R., Gorokhova, E., Salter, M. E., Ekman, A. M. L., and Bilde, M.: Influence of Arctic Microlayers and Algal Cultures on Sea Spray Hygroscopicity and the Possible Implications for Mixed-Phase Clouds, J. Geophys. Res. Atmos., 125, e2020JD032808, http://doi.org/10.1029/2020jd032808, 2020.

Cochran, R. E., Ryder, O. S., Grassian, V. H., and Prather, K. A.: Sea Spray Aerosol: The Chemical Link between the Oceans, Atmosphere, and Climate, Acc. Chem. Res., 50, 599-604, https://doi.org/10.1021/acs.accounts.6b00603, 2017.

Collins, D. B., Zhao, D. F., Ruppel, M. J., Laskina, O., Grandquist, J. R., Modini, R. L., Stokes, M. D., Russell, L. M., Bertram, T. H., Grassian, V. H., Deane, G. B., and Prather, K. A.: Direct aerosol chemical composition measurements to evaluate the physicochemical differences between controlled sea spray aerosol generation schemes, Atmos. Meas. Tech., 7, 3667-3683, 2014.

Cravigan, L. T., Mallet, M. D., Vaattovaara, P., Harvey, M. J., Law, C. S., Modini, R. L., Russell, L. M., Stelcer, E., Cohen, D. D., Olsen, G., Safi, K., Burrell, T. J., and Ristovski, Z.: Sea spray aerosol organic enrichment, water uptake and surface tension effects, Atmos. Chem. Phys., 20, 7955-7977, 2020.

Crocker, D. R., Kaluarachchi, C. P., Cao, R., Dinasquet, J., Franklin, E. B., Morris, C. K., Amiri, S., Petras, D., Nguyen, T., Torres, R. R., Martz, T. R., Malfatti, F., Goldstein, A. H., Tivanski, A. V., Prather, K. A., and Thiemens, M. H.: Isotopic Insights into Organic Composition Differences between Supermicron and Submicron Sea Spray Aerosol, Environ. Sci. Technol., 56, 9947-9958, https://doi.org/10.1021/acs.est.2c02154, 2022.

Dai, Y., Yang, S., Zhao, D., Hu, C., Xu, W., Anderson, D. M., Li, Y., Song, X.-P., Boyce, D. G., Gibson, L., Zheng, C., and Feng, L.: Coastal phytoplankton blooms expand and intensify in the 21st century, Nature, 615, 280-284, https://doi.org/10.1038/s41586-023-05760-y, 2023.

De Leeuw, G., Andreas, E. L., Anguelova, M. D., Fairall, C. W., Lewis, E. R., O'Dowd, C., Schulz, M., and Schwartz, S. E.: Production flux of sea spray aerosol, Rev. Geophys., 49, RG2001, https://doi.org/10.1029/2010RG000349, 2011.

Diamond, M. S., Gettelman, A., Lebsock, M. D., McComiskey, A., Russell, L. M., Wood, R., and Feingold, G.: To assess marine cloud brightening's technical feasibility, we need to know what to study—and when to stop, Proc. Natl. Acad. Sci. U. S. A., 119, e2118379119, 10.1073/pnas.2118379119, 2022.

Engel, A. and Händel, N.: A novel protocol for determining the concentration and composition of sugars in particulate and in high molecular weight dissolved organic matter (HMW-DOM) in seawater, Mar. Chem., 127, 180-191, https://doi.org/10.1016/j.marchem.2011.09.004, 2011.

Engel, A., Thoms, S., Riebesell, U., Rochelle-Newall, E., and Zondervan, I.: Polysaccharide aggregation as a potential sink of marine dissolved organic carbon, Nature, 428, 929-932, https://doi.org/10.1038/nature02453, 2004.

Feingold, G., Ghate, V. P., Russell, L. M., Blossey, P., Cantrell, W., Christensen, M. W., Diamond, M. S., Gettelman, A., Glassmeier, F., Gryspeerdt, E., Haywood, J., Hoffmann, F., Kaul, C. M., Lebsock, M., McComiskey, A. C., McCoy, D. T., Ming, Y., Mülmenstädt, J., Possner, A., Prabhakaran, P., Quinn, P. K., Schmidt, K. S., Shaw, R. A., Singer, C. E., Sorooshian, A., Toll, V., Wan, J. S., Wood, R., Yang, F., Zhang, J., and Zheng, X.: Physical science research needed to evaluate the viability and risks of marine cloud brightening, Sci. Adv., 10, eadi8594, 10.1126/sciadv.adi8594, 2024.

Gao, J. and Chi, J.: Biodegradation of phthalate acid esters by different marine microalgal species, Mar. Pollut. Bull., 99, 70-75, https://doi.org/10.1016/j.marpolbul.2015.07.061, 2015.

Harb, C. and Foroutan, H.: Experimental development of a lake spray source function and its model implementation for Great Lakes surface emissions, Atmos. Chem. Phys., 22, 11759-11779, https://doi.org/10.5194/acp-22-11759-2022, 2022.

Hartery, S., MacInnis, J., and Chang, R. Y.: Effect of Sodium Dodecyl Benzene Sulfonate on the Production of Cloud Condensation Nuclei from Breaking Waves, ACS Earth Space Chem., 6, 2944-2954, 2022.

Hartmann, S., Schrödner, R., Hassett, B. T., Hartmann, M., van Pinxteren, M., Fomba, K. W., Stratmann, F., Herrmann, H., Pöhlker, M., and Zeppenfeld, S.: Polysaccharides─Important Constituents of Ice-Nucleating Particles of Marine Origin, Environ. Sci. Technol., 59, 5098-5108, 10.1021/acs.est.4c08014, 2025.

Hasenecz, E. S., Kaluarachchi, C. P., Lee, H. D., Tivanski, A. V., and Stone, E. A.: Saccharide Transfer to Sea Spray Aerosol Enhanced by Surface Activity, Calcium, and Protein Interactions, ACS Earth Space Chem., 3, 2539-2548, https://doi.org/10.1021/acsearthspacechem.9b00197, 2019.

Hasenecz, E. S., Jayarathne, T., Pendergraft, M. A., Santander, M. V., Mayer, K. J., Sauer, J., Lee, C., Gibson, W. S., Kruse, S. M., Malfatti, F., Prather, K. A., and Stone, E. A.: Marine Bacteria Affect Saccharide Enrichment in Sea Spray Aerosol during a Phytoplankton Bloom, ACS Earth Space Chem., 4, 1638-1649, https://doi.org/10.1021/acsearthspacechem.0c00167, 2020.

He, J., Jiao, L., Zhi, G., Wu, X., Yang, Y., Ding, S., Zheng, J., Shao, Z., and Xia, R.: Heterogeneity of molecular-level and photochemical of dissolved organic matter derived from decomposing submerged macrophyte and algae, J. Environ. Manage., 334, 117420, https://doi.org/10.1016/j.jenvman.2023.117420, 2023.

Hu, J., Li, J., Tsona Tchinda, N., Song, Y., Xu, M., Li, K., and Du, L.: Underestimated role of sea surface temperature in sea spray aerosol formation and climate effects, npj Clim. Atmos. Sci., 7, 273, https://doi.org/10.1038/s41612-024-00823-x, 2024.

Jayarathne, T., Gamage, D. K., Prather, K. A., and Stone, E. A.: Enrichment of saccharides at the air-water interface: a quantitative comparison of sea surface microlayer and foam, Environ. Chem., 19, 506-516, https://doi.org/10.1071/EN22094, 2022.

Jayarathne, T., Sultana, C. M., Lee, C., Malfatti, F., Cox, J. L., Pendergraft, M. A., Moore, K. A., Azam, F., Tivanski, A. V., Cappa, C. D., Bertram, T. H., Grassian, V. H., Prather, K. A., and Stone, E. A.: Enrichment of Saccharides and Divalent Cations in Sea Spray Aerosol During Two Phytoplankton Blooms, Environ. Sci. Technol., 50, 11511-11520, https://doi.org/10.1021/acs.est.6b02988, 2016.

Ji, B., Singh, A., and Feng, J.: Water-to-Air Transfer of Nano/Microsized Particulates: Enrichment Effect in Bubble Bursting Jet Drops, Nano Lett., 22, 5626-5634, https://doi.org/10.1021/acs.nanolett.2c01102, 2022.

Jiang, X., Rotily, L., Villermaux, E., and Wang, X.: Submicron drops from flapping bursting bubbles, Proc. Natl. Acad. Sci. U. S. A., 119, e2112924119, https://doi.org/10.1073/pnas.2112924119, 2022.

Jiao, N., Herndl, G. J., Hansell, D. A., Benner, R., Kattner, G., Wilhelm, S. W., Kirchman, D. L., Weinbauer, M. G., Luo, T., Chen, F., and Azam, F.: Microbial production of recalcitrant dissolved organic matter: long-term carbon storage in the global ocean, Nat. Rev. Microbiol., 8, 593-599, https://doi.org/10.1038/nrmicro2386, 2010.

Kaiser, K. and Benner, R.: Biochemical composition and size distribution of organic matter at the Pacific and Atlantic time-series stations, Mar. Chem., 113, 63-77, https://doi.org/10.1016/j.marchem.2008.12.004, 2009.

Kim, S., Kramer, R. W., and Hatcher, P. G.: Graphical Method for Analysis of Ultrahigh-Resolution Broadband Mass Spectra of Natural Organic Matter, the Van Krevelen Diagram, Anal. Chem., 75, 5336-5344, https://doi.org/10.1021/ac034415p, 2003.

Labeeuw, L., Martone, P. T., Boucher, Y., and Case, R. J.: Ancient origin of the biosynthesis of lignin precursors, Biol. Direct, 10, 23, https://doi.org/10.1186/s13062-015-0052-y, 2015.

Lee, H. D., Morris, H. S., Laskina, O., Sultana, C. M., Lee, C., Jayarathne, T., Cox, J. L., Wang, X., Hasenecz, E. S., DeMott, P. J., Bertram, T. H., Cappa, C. D., Stone, E. A., Prather, K. A., Grassian, V. H., and Tivanski, A. V.: Organic Enrichment, Physical Phase State, and Surface Tension Depression of Nascent Core–Shell Sea Spray Aerosols during Two Phytoplankton Blooms, ACS Earth Space Chem., 4, 650-660, 2020.

Lhuissier, H. and Villermaux, E.: Bursting bubble aerosols, J. Fluid Mech., 696, 5-44, https://doi.org/10.1017/jfm.2011.418, 2012.

Liang, J., Ji, X., Feng, X., Su, P., Xu, W., Zhang, Q., Ren, Z., Li, Y., Zhu, Q., Qu, G., and Liu, R.: Phthalate acid esters: A review of aquatic environmental occurrence and their interactions with plants, J. Hazard. Mater., 470, 134187, https://doi.org/10.1016/j.jhazmat.2024.134187, 2024.

Lu, M., Jones, S., McKinney, M., Kandow, A., Donahoe, R., Cobb Faulk, B., Chen, S., and Lu, Y.: Assessment of phthalic acid esters plasticizers in sediments of coastal Alabama, USA: Occurrence, source, and ecological risk, Sci. Total Environ., 897, 165345, https://doi.org/10.1016/j.scitotenv.2023.165345, 2023.

Meon, B. and Kirchman, D. L.: Dynamics and molecular composition of dissolved organic material during experimental phytoplankton blooms, Mar. Chem., 75, 185-199, https://doi.org/10.1016/S0304-4203(01)00036-6, 2001.

Mühlenbruch, M., Grossart, H.-P., Eigemann, F., and Voss, M.: Mini-review: Phytoplankton-derived polysaccharides in the marine environment and their interactions with heterotrophic bacteria, Environ. Microbiol., 20, 2671-2685, https://doi.org/10.1111/1462-2920.14302, 2018.

Murphy, K., Stedmon, C., Graeber, D., and Bro, R.: Fluorescence spectroscopy and multi-way techniques. PARAFAC, Anal. Methods, 5, 6541–6882, 10.1039/c3ay41160e, 2013.

Murray, A. E., Arnosti, C., De La Rocha, C. L., Grossart, H. P., and Passow, U.: Microbial dynamics in autotrophic and

heterotrophic seawater mesocosms. II. Bacterioplankton community structure and hydrolytic enzyme activities, Aquat. Microb. Ecol., 49, 123-141, https://doi.org/10.3354/ame01139, 2007.

O'Dowd, C. D., Langmann, B., Varghese, S., Scannell, C., Ceburnis, D., and Facchini, M. C.: A combined organic-inorganic sea-spray source function, Geophys. Res. Lett., 35, http://doi.org/10.1029/2007GL030331, 2008.

Pandey, R., Usui, K., Livingstone, R. A., Fischer, S. A., Pfaendtner, J., Backus, E. H. G., Nagata, Y., Fröhlich-Nowoisky, J., Schmüser, L., Mauri, S., Scheel, J. F., Knopf, D. A., Pöschl, U., Bonn, M., and Weidner, T.: Ice-nucleating bacteria control the order and dynamics of interfacial water, Sci. Adv., 2, e1501630, 10.1126/sciadv.1501630, 2016.

Passow, U.: Transparent exopolymer particles (TEP) in aquatic environments, Prog. Oceanogr., 55, 287-333, https://doi.org/10.1016/S0079-6611(02)00138-6, 2002.

Pramanik, A., Sundararaman, M., Das, S., Ghosh, U., and Mukherjee, J.: ISOLATION AND CHARACTERIZATION OF CYANOBACTERIA POSSESSING ANTIMICROBIAL ACTIVITY FROM THE SUNDARBANS, THE WORLD'S LARGEST TIDAL MANGROVE FOREST, J. Phycol., 47, 731-743, https://doi.org/10.1111/j.1529-8817.2011.01017.x, 2011.

Quinn, P. K., Collins, D. B., Grassian, V. H., Prather, K. A., and Bates, T. S.: Chemistry and Related Properties of Freshly Emitted Sea Spray Aerosol, Chem. Rev., 115, 4383-4399, https://doi.org/10.1021/cr500713g, 2015.

Quinn, P. K., Bates, T. S., Schulz, K. S., Coffman, D. J., Frossard, A. A., Russell, L. M., Keene, W. C., and Kieber, D. J.: Contribution of sea surface carbon pool to organic matter enrichment in sea spray aerosol, Nat. Geosci., 7, 228-232, https://doi.org/10.1038/ngeo2092, 2014.

Radoman, N., Christiansen, S., Johansson, J. H., Hawkes, J. A., Bilde, M., Cousins, I. T., and Salter, M. E.: Probing the impact of a phytoplankton bloom on the chemistry of nascent sea spray aerosol using high-resolution mass spectrometry, Environ. Sci.: Atmos., 2, 1152-1169, https://doi.org/10.1039/D2EA00028H, 2022.

Rahlff, J., Stolle, C., Giebel, H.-A., Ribas-Ribas, M., Damgaard, L. R., and Wurl, O.: Oxygen Profiles Across the Sea-Surface Microlayer—Effects of Diffusion and Biological Activity, Front. Mar. Sci., Volume 6 - 2019, 2019.

Rahlff, J., Esser, S. P., Plewka, J., Heinrichs, M. E., Soares, A., Scarchilli, C., Grigioni, P., Wex, H., Giebel, H.-A., and Probst, A. J.: Marine viruses disperse bidirectionally along the natural water cycle, Nat. Commun., 14, 6354, 10.1038/s41467-023-42125-5, 2023.

Reinthaler, T., Sintes, E., and Herndl, G. J.: Dissolved organic matter and bacterial production and respiration in the sea-surface microlayer of the open Atlantic and the western Mediterranean Sea, Limnol. Oceanogr., 53, 122-136, https://doi.org/10.4319/lo.2008.53.1.0122, 2008.

Rinaldi, M., Fuzzi, S., Decesari, S., Marullo, S., Santoleri, R., Provenzale, A., von Hardenberg, J., Ceburnis, D., Vaishya, A., O'Dowd, C. D., and Facchini, M. C.: Is chlorophyll-a the best surrogate for organic matter enrichment in submicron primary marine aerosol?, J. Geophys. Res. Atmos., 118, 4964-4973, https://doi.org/10.1002/jgrd.50417, 2013.

Rocchi, A., von Jackowski, A., Welti, A., Li, G., Kanji, Z. A., Povazhnyy, V., Engel, A., Schmale, J., Nenes, A., Berdalet, E., Simó, R., and Dall′Osto, M.: Glucose Enhances Salinity-Driven Sea Spray Aerosol Production in Eastern Arctic Waters, Environ. Sci. Technol., 58, 8748-8759, https://doi.org/10.1021/acs.est.4c02826, 2024.

Santander, M. V., Schiffer, J. M., Lee, C., Axson, J. L., Tauber, M. J., and Prather, K. A.: Factors controlling the transfer of biogenic organic species from seawater to sea spray aerosol, Sci. Rep., 12, 3580, https://doi.org/10.1038/s41598-022-07335-9, 2022.

Santander, M. V., Malfatti, F., Pendergraft, M. A., Morris, C., Kimble, K. L., Mitts, B. A., Wang, X., Mayer, K. J., Sauer, J., Lee, C., and Prather, K. A.: Bacterial Control of Marine Humic-Like Substance Production, Composition, Size, and Transfer to Sea Spray Aerosols During Phytoplankton Blooms, J. Geophys. Res. Atmos., 128, e2022JD036869, https://doi.org/10.1029/2022jd036869, 2023.

Schill, S. R., Burrows, S. M., Hasenecz, E. S., Stone, E. A., and Bertram, T. H.: The Impact of Divalent Cations on the Enrichment of Soluble Saccharides in Primary Sea Spray Aerosol, Atmosphere, 9, 476, 2018.

Schmitt-Kopplin, P., Liger-Belair, G., Koch, B. P., Flerus, R., Kattner, G., Harir, M., Kanawati, B., Lucio, M., Tziotis, D., Hertkorn, N., and Gebefügi, I.: Dissolved organic matter in sea spray: a transfer study from marine surface water to aerosols, Biogeosciences, 9, 1571-1582, 10.5194/bg-9-1571-2012, 2012.

Schum, S. K., Brown, L. E., and Mazzoleni, L. R.: MFAssignR: Molecular formula assignment software for ultrahigh resolution mass spectrometry analysis of environmental complex mixtures, Environ. Res., 191, 110114, https://doi.org/10.1016/j.envres.2020.110114, 2020.

Sellegri, K., O'Dowd, C. D., Yoon, Y. J., Jennings, S. G., and De Leeuw, G.: Surfactants and submicron sea spray generation, J. Geophys. Res., 111, D22215, https://doi.org/10.1029/2005jd006658, 2006.

Song, Y., Li, J., Tsona Tchinda, N., Li, K., and Du, L.: Role of sea spray aerosol at the air–sea interface in transporting aromatic acids to the atmosphere, Atmos. Chem. Phys., 24, 5847-5862, https://doi.org/10.5194/acp-24-5847-2024, 2024.

Stedmon, C. A. and Bro, R.: Characterizing dissolved organic matter fluorescence with parallel factor analysis: a tutorial, Limnol. Oceanogr. Meth., 6, 572-579, https://doi.org/10.4319/lom.2008.6.572, 2008.

Stokes, M. D., Deane, G. B., Prather, K., Bertram, T. H., Ruppel, M. J., Ryder, O. S., Brady, J. M., and Zhao, D.: A Marine Aerosol Reference Tank system as a breaking wave analogue for the production of foam and sea-spray aerosols, Atmos. Meas. Tech., 6, 1085-1094, https://doi.org/10.5194/amt-7-3667-2014, 2013.

Stokes, M. D., Deane, G., Collins, D. B., Cappa, C., Bertram, T., Dommer, A., Schill, S., Forestieri, S., and Survilo, M.: A miniature Marine Aerosol Reference Tank (miniMART) as a compact breaking wave analogue, Atmos. Meas. Tech., 9, 4257-4267, https://doi.org/10.5194/amt-9-4257-2016, 2016.

Suo, C., Zhao, W., Liu, S., Ren, Y., Zhang, Y., Qiu, Y., and Wu, F.: Molecular insight into algae-derived dissolved organic matters via Fourier-transform ion cyclotron resonance mass spectrometry: Effects of pretreatment methods and electrospray ionization modes, J. Hazard. Mater., 480, 136220, https://doi.org/10.1016/j.jhazmat.2024.136220, 2024.

Tammaro, D., Chandran Suja, V., Kannan, A., Gala, L. D., Di Maio, E., Fuller, G. G., and Maffettone, P. L.: Flowering in bursting bubbles with viscoelastic interfaces, Proc. Natl. Acad. Sci. U. S. A., 118, e2105058118, https://doi.org/10.1073/pnas.2105058118, 2021.

Thornton, D. C. O.: Dissolved organic matter (DOM) release by phytoplankton in the contemporary and future ocean, Eur. J. Phycol., 49, 20-46, 10.1080/09670262.2013.875596, 2014.

Triesch, N., van Pinxteren, M., Engel, A., and Herrmann, H.: Concerted measurements of free amino acids at the Cabo Verde islands: high enrichments in submicron sea spray aerosol particles and cloud droplets, Atmos. Chem. Phys., 21, 163-181, https://doi.org/10.5194/acp-21-163-2021, 2021a.

Triesch, N., van Pinxteren, M., Salter, M., Stolle, C., Pereira, R., Zieger, P., and Herrmann, H.: Sea Spray Aerosol Chamber Study on Selective Transfer and Enrichment of Free and Combined Amino Acids, ACS Earth Space Chem., 5, 1564-1574, https://doi.org/10.1021/acsearthspacechem.1c00080, 2021b.

Tumminello, P. R., Niles, R., Valdez, V., Madawala, C. K., Gamage, D. K., Kimble, K. L. A., Leibensperger, R. J., III, Huang, C., Kaluarachchi, C., Dinasquet, J., Malfatti, F., Lee, C., Deane, G. B., Stokes, M. D., Stone, E., Tivanski, A., Prather, K. A., Boor, B. E., and Slade, J. H.: Size-Dependent Nascent Sea Spray Aerosol Bounce Fractions and Estimated Viscosity: The Role of Divalent Cation Enrichment, Surface Tension, and the Kelvin Effect, Environ. Sci. Technol., 58, 19666-19678, https://doi.org/10.1021/acs.est.4c04312, 2024.

Tyree, C. A., Hellion, V. M., Alexandrova, O. A., and Allen, J. O.: Foam droplets generated from natural and artificial seawaters, J. Geophys. Res., 112, 10.1029/2006jd007729, 2007.

Vaishya, A., Ovadnevaite, J., Bialek, J., Jennings, S. G., Ceburnis, D., and O'Dowd, C. D.: Bistable effect of organic enrichment on sea spray radiative properties, Geophys. Res. Lett., 40, 6395-6398, https://doi.org/10.1002/2013GL058452, 2013.

Veron, F.: Ocean Spray, Annu. Rev. Fluid Mech., 47, 507-538, https://doi.org/10.1146/annurev-fluid-010814-014651, 2015.

Villacorte, L. O., Ekowati, Y., Neu, T. R., Kleijn, J. M., Winters, H., Amy, G., Schippers, J. C., and Kennedy, M. D.: Characterisation of algal organic matter produced by bloom-forming marine and freshwater algae, Water Res., 73, 216-230, https://doi.org/10.1016/j.watres.2015.01.028, 2015.

Wan, Y., Xing, C., Wang, X., Yang, Z., Huang, X., Ge, X., Du, L., Wang, Q., and Yu, H.: Nontarget Tandem High-Resolution Mass Spectrometry Analysis of Functionalized Organic Compounds in Atmospherically Relevant Samples, Environ. Sci. Technol. Lett., 9, 1022-1029, 10.1021/acs.estlett.2c00788, 2022.

Wang, X., Deane Grant, B., Moore Kathryn, A., Ryder Olivia, S., Stokes, M. D., Beall Charlotte, M., Collins Douglas, B., Santander Mitchell, V., Burrows Susannah, M., Sultana Camille, M., and Prather Kimberly, A.: The role of jet and

film drops in controlling the mixing state of submicron sea spray aerosol particles, Proc. Natl. Acad. Sci. U. S. A., 114, 6978-6983, https://doi.org/10.1073/pnas.1702420114, 2017.

Wang, X., Sultana, C. M., Trueblood, J., Hill, T. C. J., Malfatti, F., Lee, C., Laskina, O., Moore, K. A., Beall, C. M., McCluskey, C. S., Cornwell, G. C., Zhou, Y., Cox, J. L., Pendergraft, M. A., Santander, M. V., Bertram, T. H., Cappa, C. D., Azam, F., DeMott, P. J., Grassian, V. H., and Prather, K. A.: Microbial Control of Sea Spray Aerosol Composition: A Tale of Two Blooms, ACS Cent. Sci., 1, 124-131, https://doi.org/10.1021/acscentsci.5b00148, 2015.

Wang, Z. and Liu, L.: Effect of film characteristics on bursting behavior of a bubble in gas space, Chem. Eng. Sci., 307, 121355, https://doi.org/10.1016/j.ces.2025.121355, 2025.

Xu, M. L., Tchinda, N. T., Li, J. L., and Du, L.: Insoluble lipid film mediates transfer of soluble saccharides from the seato the atmosphere: the role of hydrogen bonding, Atmos. Chem. Phys., 23, 2235-2249, https://doi.org/10.5194/acp-23-2235-2023, 2023.

Xu, M. L., Tchinda, N. T., Li, S. Y., and Du, L.: Enhanced saccharide enrichment in sea spray aerosols by coupling surface-active fatty acids, Sci. Total Environ., 916, 170322, https://doi.org/10.1016/j.scitotenv.2024.170322, 2024.

Xu, W., Ovadnevaite, J., Fossum, K. N., Lin, C., Huang, R.-J., Ceburnis, D., and O'Dowd, C.: Sea spray as an obscured source for marine cloud nuclei, Nat. Geosci., 15, 282-286, https://doi.org/10.1038/s41561-022-00917-2, 2022.

Zhang, Z., Chen, Y., Wang, R., Cai, R., Fu, Y., and Jiao, N.: The Fate of Marine Bacterial Exopolysaccharide in Natural Marine Microbial Communities, PloS one, 10, e0142690, https://doi.org/10.1371/journal.pone.0142690, 2015.

Zhong, X. and Ran, X.: Deciphering and quantifying nitrate sources and processes in the central Yellow Sea using dual isotopes of nitrate, Water Res., 261, 121995, https://doi.org/10.1016/j.watres.2024.121995, 2024.